

Multiplet structure in Pu-based compounds: A photoemission case study of PuSi_x ($0.5 \leq x \leq 2$) films

T. Gouder,* R. Eloirdi, J. Rebizant, P. Boulet, and F. Huber

European Commission, Joint Research Centre, Institute for Transuranium Elements, Postfach 2340, D-76125 Karlsruhe, Germany

(Received 13 October 2004; published 1 April 2005)

Thin films of PuSi_x ($0.5 \leq x \leq 2$) were prepared by sputter deposition and studied by x-ray and ultraviolet photoelectron spectroscopy. Photoemission of the Pu $4f$ core levels and the Pu $5f$ valence band states showed first a breakdown of $5f$ band behavior at low Si content, but then an increasing tendency for $5f$ hybridization for more diluted PuSi_x systems. In valence band spectra, a broad peak at high binding energy is observed for concentrated systems (PuSi). It is replaced by a sharp three-peak structure close to the Fermi level for more diluted systems (PuSi_2). Both structures are discussed in terms of final-state multiplets of localized $5f$ states with different degrees of hybridization. It is concluded that multiplets and final-state effects occur quite generally in Pu systems and explain many of the spectral features, which often have been ascribed to the ground-state density of state.

DOI: 10.1103/PhysRevB.71.165101

PACS number(s): 71.20.Gj, 71.28.+d

I. INTRODUCTION

The physics of plutonium and its compounds is dominated by the competition between $5f$ itinerancy associated with chemical bonding and $5f$ on-site localization. Pu has a particular position within the actinide series. It is the last element where the $5f$ electrons still participate in bonding, while in the next element, Am, they retract from bonding and become localized. The delicate balance between itinerancy and localization is quite sensitive to slight variations in the chemical environment. The existence of six allotropic phases (α to δ) in a narrow temperature range,¹ the substantial drop in density (by 20%) between the room temperature α - and the high temperature δ -Pu, and the localization of the $5f$ states when Pu is confined to thin films^{2,4} are direct consequences of the weak bonding properties of the $5f$ states.

Over the last 20 years, the electronic structure of Pu metal (α and δ) has been widely investigated by photoemission spectroscopy.^{2,4–8,10} Valence band data have been compared to theoretical calculations, and good correspondence between them and the calculated ground-state density of states (DOS) has been taken as an indication for the validity of the theoretical model [dynamical mean field theory,¹¹ constrained local density approximation (LDA), or a “mixed level model” with four of the five $5f$ states forced into localization,^{8,12,13} and LDA+ U (Ref. 14)]. In this approach, it was generally implied that photoemission itself represents one well-defined final state, which then can be related to the ground state. Competing final states (with good or poor screening) would not occur in the valence band spectra. However, for the $4f$ core-level spectra of Pu, these competing final states exist, and are directly related to the narrow-band nature of Pu.⁶ Therefore, similar final effects should occur in the valence band spectra and superimpose on the ground-state DOS features. These effects should become more important when the $5f$ states approach localization. In this paper we want to address this issue and present a photoemission study of the Pu-Si series, where the $5f$ itinerancy is modified by diluting Pu with a ligand element. We will argue that the spectra

show band features together with localized $5f$ states, appearing as final-state multiplets. Coexistence of these does not reflect a mixed level ground state, but is due to final-state screening effects as for the $4f$ core levels. The discussion will be extended to other Pu systems.

The electronic structure of Pu in the silicide series is determined by two opposing effects. On the one hand, dilution of Pu in a Si matrix favors $5f$ localization, because the direct $5f$ - $5f$ overlap of neighboring Pu atoms is suppressed. Above a critical distance (the Hill limit, 0.34 nm for Pu) the overlap is too weak to enable $5f$ band formation. On the other hand, the bonding interaction between Pu and the Si ligand atoms favors hybridization between the Pu $5f$ and the Si $3p$ states, and thus could itself result in $5f$ delocalization. Replacement of the pure f conduction band by an f ligand hybrid band is at the base of heavy-fermion materials in the actinides and lanthanides,¹⁵ where the f -atom separation is significantly greater than the Hill limit. It was not clear, *a priori*, which of the two effects would dominate and whether or not the $5f$ states would become localized at high dilution. In this context, comparison with the Ce-Si system is instructive. As in Pu, f states in Ce are close to the localization threshold and there are strong similarities between the physics of these two elements.¹⁶ CeSi_x ($1.6 \leq x \leq 2$) has been studied by photoemission and magnetic measurements.¹⁷ The more concentrated CeSi_x was found to be closer to localization than the dilute, suggesting that ligand hybridization effects prevail over dilution effects. High-resolution photoemission data show a sharp emission right at the Fermi level, a peak at 0.3 eV binding energy (BE), and a large peak at 2.5 eV BE. These data are interpreted either in the framework of the single-impurity model,¹⁷ or in terms of different final-state screening channels.¹⁸ Both models attribute the peak at 2.5 eV to the localized response (the $4f^1 \rightarrow 4f^0$ transition), and the structures close to the Fermi level to some type of hybridized response, be it the Kondo resonance with its spin-orbit (SO) sideband, or the ordinary SO split $5f$ peak,^{19,20} which corresponds to the f^1 final-state configuration. Below we will show that a very similar interpretation can be applied to the Pu-Si system.

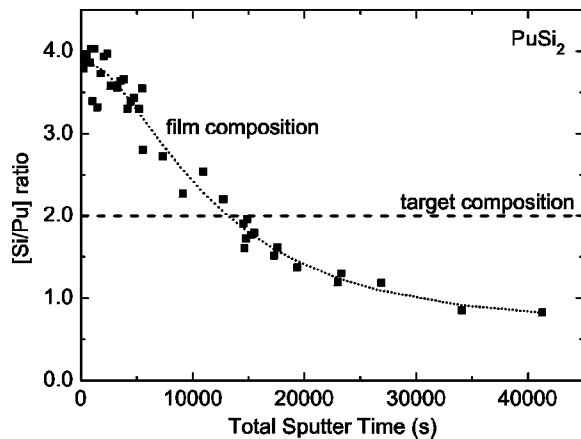


FIG. 1. Evolution of the film composition ($[\text{Si}]/[\text{Pu}]$ ratio) with the total sputter time for the PuSi_2 target. The horizontal line ($[\text{Si}]/[\text{Pu}] = 2$) shows the target composition. After initial enrichment (PuSi_4) the Si content of the films drops below that of the target and settles at a final film composition of $\text{PuSi}_{0.7}$.

II. EXPERIMENT

Thin layers of PuSi_x ($0.5 \leq x \leq 2$) were prepared *in situ* by dc sputtering in an Ar atmosphere (2–20 Pa Ar, Pu target at -700 V) from PuSi and PuSi_2 targets. The plasma in the diode source was maintained by injection of electrons of 50–100 eV energy. As sputter gas we used ultrahigh-purity Ar (99.9999%). The deposition rate was about one monolayer per second and the deposition time was 100 s. The PuSi and PuSi_2 targets were air cooled. The substrate was also kept at room temperature. The targets were small rods of stoichiometric silicides (1.5 mm diameter, 8 mm length), which were cleaned before introduction into the vacuum chamber by mechanical polishing. The background pressure of the plasma chamber was 4×10^{-7} Pa. For the spectroscopy experiments, we used a single-crystalline Mo (100) substrate, which was cleaned *in situ* by Ar ion sputtering at $T=673$ K. The deposition currents were typically 1–2 mA.

Photoelectron spectra were recorded using a Leybold LHS-10 hemispherical analyzer. X-ray photoelectron spectra (XPS) were taken using Al $K\alpha$ (1486.6 eV) radiation with an approximate resolution of 1 eV. Ultraviolet photoelectron spectroscopy (UPS) measurements were made using He I and He II ($h\nu=21.22$ and 40.81 eV) excitation produced by a high-density plasma uv source (SPECS). The total resolution in UPS was 0.1–0.05 eV for the high-resolution scans. The background pressure in the analysis chamber was better than 10^{-8} Pa.

The film composition was determined from the ratio of the Pu $4f_{7/2}$ and the Si $2s$ peak areas.⁹ For the PuSi_2 target the composition of the films changed during the deposition process (Fig. 1). Initially the films were enriched in Si. Then the Si content dropped with time below the nominal composition of the target and settled at a final value of $\text{PuSi}_{0.8}$. The initial enrichment and the drop below the target composition are explained by the preferential sputtering of Si.²¹ Depletion was slow enough that film composition remained constant for each deposition run. The PuSi_x films produced by sputter deposition are mostly off stoichiometric. Nevertheless they

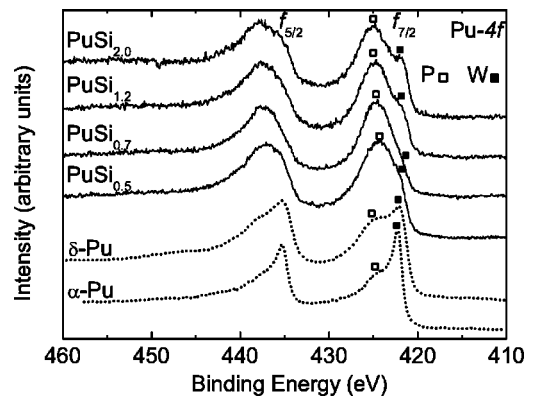


FIG. 2. Pu $4f$ core-level spectra of α -Pu, δ -Pu, and PuSi_x ($0.5 \leq x \leq 2.0$). The poorly screened peak (P) appears as a satellite in α -Pu, grows in intensity in δ -Pu, and is dominant in all PuSi_x films.

can be assumed to be homogeneous, because in the plasma, atomic intermixing takes place and the huge quenching rate after condensation on the surface prevents phase separation. This allows us to study the evolution of the electronic structure as a continuous function of Pu dilution.

In this paper we label the films by PuSi_x , instead of the more generally used Pu_aSi_b (a and b given in atomic percent). Thus $\text{PuSi}_{0.5}$ corresponds to $\text{Pu}_{66}\text{Si}_{33}$. By using this designation, we do not imply formation of well-defined phases for the films. But we use this label for easier comparison between the films and the stoichiometric bulk compounds, on which magnetic measurements have been performed.

III. RESULTS

A. Core-level study

Figure 2 shows the Pu $4f$ core-level lines of PuSi_x systems for increasing Si concentration, together with α - and δ -Pu reference spectra. The two characteristic spin-orbit split peaks ($4f_{5/2}$ and $4f_{7/2}$) are centered at about 436 and 423 eV binding energy, respectively. α -Pu is the most itinerant system of this series. Its $4f$ emissions appear as a strong, sharp main line labeled W at low BE (423 eV for $4f_{7/2}$) accompanied by small satellites labeled P at 2 eV higher BE. In δ -Pu the main line W is suppressed while the satellite P becomes more pronounced. Interpretation is straightforward in terms of the final-state screening concept.²² The peak W belongs to the final state screened by occupation of $5f$ levels (well screened), which implies their hybridization with conduction or valence band states. Therefore the probability of this screening channel is larger for the itinerant α -Pu than for the more localized δ -Pu. The peak P is attributed to the d -screened final state (poorly screened), which occurs if the f -screening channel is closed—notably when the f states are less hybridized. α - and δ -Pu spectra thus simply show that approaching localization is reflected in the final-state screening processes, which lead to the replacement of the well-screened (W) by the poorly screened (P) peak.

For all PuSi_x systems, the poorly screened peak P clearly dominates the well-screened peak W , and it is concluded that

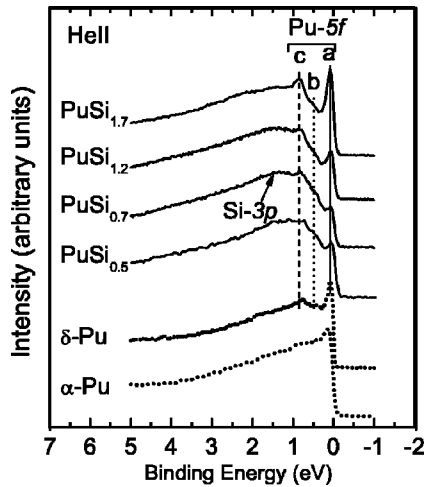


FIG. 3. He II valence band spectra of α -Pu, δ -Pu, and PuSi_x ($0.5 \leq x \leq 1.7$).

the $5f$ states in these compounds are essentially localized. The poorly screened $4f$ peak is significantly broader than the well-screened peak. This is attributed to the exchange interaction between the $4f$ core-hole and localized $5f$ states,²³ and thus provides additional evidence for $5f$ localization in this final state. The evolution of the well-screened peak is quite remarkable. At low Si content ($\text{PuSi}_{0.5}$) it is weak and not well resolved from the poorly screened peak. It then disappears in $\text{PuSi}_{0.7}$, but reappears gradually for more diluted system, being now better separated from the poorly screened peak P , and settles at a maximal intensity for PuSi_2 . Since the well-screened peak W is related to the hybridization of the $5f$ states with extended states, it should be concluded that this hybridization passes through a minimum around $\text{PuSi}_{0.7}$. Below the minimum, hybridization is mainly due to direct $5f$ - $5f$ overlap, and therefore it is suppressed when Si atoms are added. Above the minimum, hybridization is due to the mixing of the f states with ligand states, and thus it becomes more pronounced with higher Si concentration. It is strong enough to outweigh the dilution effects.

B. Valence band study

The He II valence band spectra of PuSi_x ($0.5 \leq x \leq 2.0$) are displayed in Fig. 3 and compared to α -Pu and δ -Pu spectra. In He II the Pu $5f$ cross section is about 30 times larger than that of Si $3p$.²⁴ The valence band spectra of the PuSi_x series are thus dominated by the Pu $5f$ lines. In α -Pu there is a broad $5f$ band with the maximum at the Fermi level. The band is featureless except for a small shoulder at 0.8 eV binding energy. The $5f$ states in this material are well itinerant, and the valence band looks very similar to those of Np or U. The triangular shape is qualitatively explained by the rising edge of a less than half-filled band, which is cut by the Fermi level. In δ -Pu, the broad triangular shape is disrupted, and a weak gap appears at 0.1 eV BE. This gap is part of a three-peak structure (a , b , and c peaks), which is found in several Pu systems^{2,4} and consists of the sharp peak right at the Fermi level (labeled a), and two peaks at about 0.5 (la-

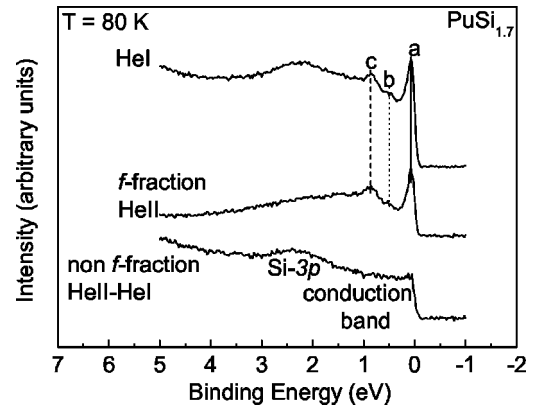


FIG. 4. He I and He II spectra of $\text{PuSi}_{1.7}$ measured at 80 K. In He I the Pu $5f$ cross section is strongly suppressed, and the non- f features become visible. The broad Si $3p$ peak in PuSi_2 testifies to the presence of Si. By subtracting the He II spectra from He I, all components (a , b , and c) of the f emission disappear. This shows that they all are purely f -like.

beled b) and 0.85 eV (labeled c) binding energy. The component at 0.5 eV is very weak, but it is reproducible. Quite remarkably, the $5f$ -band narrowing, which should accompany the volume expansion from α - to δ -Pu, does not appear in the valence band spectra. The $5f$ signal has the same width of about 4 eV for both allotropes. Only the appearance of the three-peak structure and among them the appearance of the sharp resonance at the Fermi level may be reminiscent of the narrowing. It scales qualitatively with the increase of the electronic specific heat, from $22 \text{ mJ mol}^{-1} \text{ K}^{-2}$ in α -Pu to $53 \text{ mJ mol}^{-1} \text{ K}^{-2}$ in δ -Pu.²⁵

In $\text{PuSi}_{0.5}$ the emission at the Fermi level is strongly suppressed, and the main spectral intensity is found in the broad peak above 1 eV binding energy. The spectrum looks similar to that of PuSb ,³ which has localized $5f$ states with a $5f^5$ configuration. The small peak at the Fermi level decreases even further in $\text{PuSi}_{0.7}$. It is part of the three-peak structure, already observed in δ -Pu. Initially it is weak, but from $\text{PuSi}_{1.2}$ on, it increases again and becomes a strong resonance in $\text{PuSi}_{1.7}$.

Further identification of the peaks in the valence region is achieved by comparing He II and He I spectra. In He I the cross section of the $5f$ emission is suppressed by a factor of 6,²⁴ while the $6d$ cross section increases by a factor of about 4. In a good approximation, the He II spectrum can be regarded as a pure f spectrum. The dominating three-peak structure in He II is thus mainly of f character. The f and non- f contributions in the He I spectrum can then be separated by subtracting the He II spectrum (Fig. 4). After subtracting all three peaks disappear simultaneously. This proves that they all have the same f character, and none of them has d admixture as would happen in the case of f - d hybridization. They leave a flat region between 0 and 1 eV, which represents the (non- f) conduction band cut by the Fermi energy. The broad peak around 2 eV binding energy is attributed to the Si $3p$ level. It becomes more pronounced in He I, because its cross section stays constant while the f emissions are suppressed.

IV. DISCUSSION

The Pu-Si series was studied to follow the evolution of the Pu $5f$ photoemission spectra with gradual f localization. We were interested in how non-ground-state features, which become more pronounced for more localized states, influence the spectra. This is relevant for most Pu metallic compounds.

Within the PuSi_x series, the nature of the $5f$ states is determined by the opposing effects of dilution (favoring localization) and $5f$ -ligand-state hybridization (favoring itinerancy). There are five known Pu-Si phases, which are stable at room temperature: Pu_5Si_3 ($=\text{PuSi}_{0.6}$), Pu_3Si_2 ($=\text{PuSi}_{0.7}$), PuSi , Pu_3Si_5 ($=\text{PuSi}_{1.7}$), PuSi_2 . Recent investigation of the magnetic properties²⁶ showed that PuSi orders ferromagnetically around 72 K with a local and effective moment of $0.72\mu_B$. PuSi_2 was shown to be a Curie-Weiss paramagnet with a local and effective moment of $0.54\mu_B$. The Pu-Pu distances in PuSi and PuSi_2 are 0.364 and 0.397 nm, which is above the Hill limit. This favors $5f$ localization, and one would expect a $5f^5$ configuration. However the moments are reduced compared to the theoretical value of $0.86\mu_B$ (intermediate coupling) for the $5f^5$ configuration in the free ion. The stronger suppression of the local moment in dilute PuSi_2 relative to PuSi points to a stronger hybridization of the localized $5f$ states in PuSi_2 , resulting in partial shielding of the moment. The existence of a localized $5f^5$ ground-state configuration with different degree of residual f hybridization explains very well the photoemission spectra, as will be shown below.

A. Core-level and valence band spectroscopy

The existence of different final states (well and poorly screened) in core-level spectroscopy is often encountered in narrow-band materials.²⁷ It is related to the difficulty of narrow-band states in screening the core hole, so that screening is performed partially by more extended (conduction band) states. Qualitatively, the decrease of the intensity of the well-screened peak W relative to the poorly screened peak P (Fig. 2) is an indication for decreasing hybridization of the $5f$ states. There is no sharp transition upon localization in the ground state, but photoemission spectra of itinerant systems already show the poorly screened (localized) response, e.g., α -Pu,⁶ while clearly localized systems, e.g., Am,²² still show the well-screened (hybridized) final state, appearing as a low-intensity shoulder. In $\text{PuSi}_{0.7}$ the well-screened $4f$ peak (W) virtually disappeared. The $5f$ states thus are only weakly hybridized, and even in the ground state $5f$ localization is expected. In $\text{PuSi}_{1.2}$, the well-screened peak grows again. It reaches a similar intensity as that of the well-screened peak in americium metal.²² Am metal, however, has a localized ground state, and this suggests that also in $\text{PuSi}_{1.7}$ the $5f$ states are localized. Therefore, the $5f$ spectra should not be discussed in terms of a $5f$ band (i.e., compared to the ground-state DOS), but instead they reflect final-state effects for localized $5f$ levels with different degree of hybridization.

B. The $5f$ multiplet

Photoemission from localized levels leads to final-state multiplets, which are characteristic for the ground-state

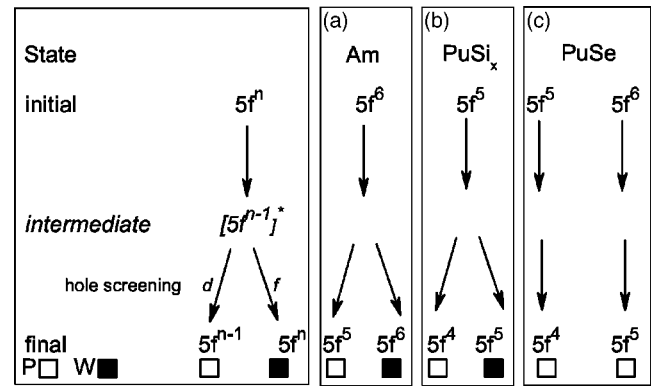


FIG. 5. Initial and final f configurations in actinide compounds: Am metal, PuSi_x , and PuSe . In Am and PuSi_x the ground state leads to the well-screened (W) and to the poorly screened (P) final states. For PuSe , known for intermediate valence, only the poorly screened final state is reached.

configuration.²⁸ Among the light actinides, Am is the first element with (weakly) localized $5f$ states. It displays such multiplets, and can be taken as reference. Photoemission from the ground-state Am $5f^6$ configuration leads to two final states [Fig. 5(a)],²⁹ screened either by an f state (well-screened, W) or by a d state (poorly screened, P). The final states appear with the characteristic $5f^6$ and $5f^5$ multiplet structures,²⁹ which for actinides are obtained within the intermediate coupling scheme.³⁰ It is important to notice that even the well-screened peak, where the f hole is screened by an f state, does not correspond to the ground state, but appears as a final-state multiplet structure.

A similar model can be applied to PuSi_x [Fig. 5(b)], just by changing the initial-state configuration to $5f^5$. Photoemission then leads to two final states, the well-screened (W) $5f^5$ and the poorly screened (P) $5f^4$. The corresponding multiplets should be consistent with those calculated in the intermediate coupling scheme,³⁰ which was shown recently to be applicable to Pu.³¹ These multiplets must appear in other Pu compounds with localized $5f$ states. The $5f^4$ multiplet should be pronounced for weakly hybridized f states (strong localization), where the poorly screened final state dominates, and the $5f^5$ multiplet for more hybridized f states (weak localization).

1. $5f^4$ multiplet

Figure 6 compares spectra of the strongly localized $\text{PuSi}_{0.7}$, PuSb ,³ and Pu_2O_3 . PuSb is the prototype of a weakly hybridized Pu compound. It has an effective moment of $0.86\mu_B$, which is virtually identical with the free ion $5f^5$ value. Pu_2O_3 is an ionic compound (weak hybridization), with Pu at an oxidation state of +3 ($5f^5$). The $4f$ core-level spectra for all three compounds show the poorly screened peak, thus confirming weak hybridization. So for all three compounds the $5f$ spectrum should be dominated by the $5f^4$ final-state multiplet. Indeed, all three compounds show a broad emission around 2 eV binding energy, which by comparison of He I and He II spectra are identified as f levels (the weak three-peak structure in $\text{PuSi}_{0.7}$ will be discussed be-

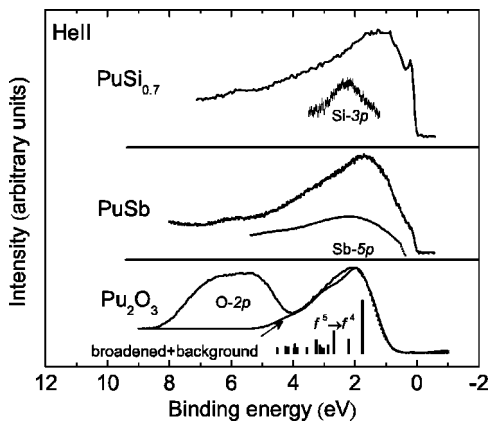


FIG. 6. He II spectra of strongly localized Pu compounds: PuSi_{0.7}, PuSb, and Pu₂O₃. Also the calculated $5f^5 \rightarrow 5f^4$ multiplet transition is shown, together with the synthetic curve after adding lifetime-dependent broadening and inelastic background.

low). The corresponding $5f^4$ multiplet ($5f^5 \rightarrow 5f^4$ transition),³⁰ displayed with the Pu₂O₃ spectrum, fits the experimental spectra very well. Due to considerable lifetime broadening, the individual terms are not resolved. Similar broadening also occurs in the spectrum of Am metal.²⁹ The lifetime is determined by the Auger decay rate of the final-state hole, which proceeds via transfer of electrons from the valence band. It is particularly strong when the $5f^4$ multiplet overlaps with the valence or conduction band.³² This explains that these lifetime effects are material dependent, and the $5f^4$ signal is broader in PuSb with a low-lying valence band (Sb 5p; see Fig. 6) than in Pu₂O₃ with the O 2p valence band at high binding energy.

2. $5f^5$ multiplet

The $5f^5$ final-state multiplet appears as a characteristic three-peak structure close to the Fermi level (Fig. 7). It is found in very different systems (PuSi_{1.7}, PuSe, δ -Pu), and we argue that in all these systems the same $5f^5$ final state is reached. The corresponding ($5f^6 \rightarrow 5f^5$) multiplet transition³⁰ reproduces the experimental features very well. The multiplet terms are better resolved than for the $5f^4$ final state. This can be explained by the longer lifetime of a shallow hole.³² For PuSi_{1.7}, the $5f^5$ final state can thus be attributed to good screening. It shows that the f states are more strongly hybridized relatively to PuSi. This is consistent with the evolution of the well-screened peak W in the $4f$ spectrum (Fig. 2) and the lowered magnetic moment in PuSi₂.

C. Intermediate valence and final-state multiplets

The three-peak structure also appears in PuSe (Fig. 7), together with a broad f peak around 2 eV binding energy, and a straightforward explanation in terms of a $5f^5$ and $5f^4$ final state can be given. PuSe is an intermediate valence system,³³ which in the ground state has a mixed $5f^5/5f^6$ configuration. The f states are only weakly hybridized, so that photoemission always leads to the poorly screened final states [Fig. 5(c)].

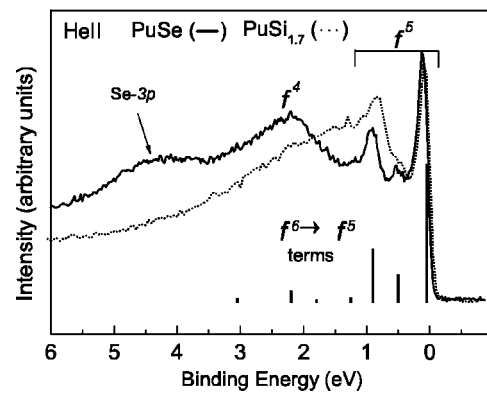


FIG. 7. He II valence band spectra of PuSi_{1.7} and PuSe, showing the characteristic three-peak structure at the Fermi level. Also the calculated $5f^6 \rightarrow 5f^5$ multiplet transition is displayed.

The $5f^4$ and $5f^5$ final states then correspond to the $5f^5$ and $5f^6$ configurations in the ground state. They thus do not reflect two different screening mechanisms (as in PuSi_x), but the mixed ground-state configuration of an intermediate valence system.

D. The case of δ -Pu metal and Pu thin films

For δ -Pu a similar three-peak structure superimposes onto the broad f emission (Fig. 3). It is related to the approaching localization, because it is more pronounced in δ - than in α -Pu. Nevertheless, it is generally interpreted in terms of ground-state density of states.^{8,11-14} We think instead that it contains the final-state multiplet structure of a localized $5f^5$ configuration, which superimposes on the bandlike response. The existence of an excited final state is indeed suggested by the well- and poorly screened components in the $4f$ core level spectra (Fig. 2). They show that the $5f$ states in Pu are not itinerant enough to screen the core hole alone. Therefore, they do not perfectly screen the $5f$ hole either, and the $5f$ spectrum in Pu metal is a superposition of the localized $5f^5$ final state, responsible for the three-peak structure, and the itinerant states, responsible for the broad triangular background peak. In α -Pu, the itinerant response is strong, because the $5f$ states are more delocalized, and the three-peak structure becomes weak. In δ -Pu, $5f$ hybridization is weakened, but still significantly larger than in PuSi_{2.0}, as shown by the strong size of the well-screened core-level peak. In the valence band spectra of δ -Pu,¹³ the stronger f - d hybridization is shown by the enhanced d character of the peak right at the Fermi level: this peak is less suppressed in He I than the two other components at 0.5 and 0.85 eV binding energy, while for PuSi_{1.7} (Fig. 4), all three peaks are suppressed. Thus there is a gradual evolution from the itinerant α -Pu, over δ -Pu, to PuSi₂. Such interpretation is supported by the behavior of Pu films.^{2,4} Thick films have fairly itinerant f states, and their spectra are intermediate between those of α - and δ -Pu. With decreasing film thickness, the spectra evolve from the itinerant to the localized $5f^5$ response (with still hybridized $5f$ states), and eventually reach the $5f^4$ final-state response (with weakly hybridized $5f$ states), thus spanning the entire range from itinerancy to complete localization. The

special situation where photoemission from a weakly itinerant ground state leads to a localized final state has been encountered previously for the uranium pnictides (UP, UAs), where a narrow band exists in the ground state (large γ coefficient of the specific heat), but photoemission gives a characteristic multiplet structure.³⁴

E. The Ce-Pu analogy

A very similar picture has been applied to Ce which, like Pu, has weakly itinerant f electrons in the ground state. The corresponding ground-state configurations are close to Ce $4f^1$ and Pu $5f^5$ (the exact f count is not integer and depends on the allotropic phase).

Taking this difference into account, photoemission spectra can be interpreted along similar lines. The $4f^1$ final state in Ce corresponds to the $5f^5$ final state in Pu. It may be reached from the narrow band in the ground state, and leads to the $^{5/2}F$ and $^{7/2}F$ doublet at the Fermi level, observed in α -Ce.^{19,20} The $4f^0$ final state in Ce corresponds to the $5f^4$ final state in Pu. As in Pu, this final state is strongly broadened, and again can be explained by the lifetime effects. Also the silicides of Pu and Ce behave similarly. In CeSi_x the hybridized response becomes more pronounced with higher Si content. In photoemission, the $4f^1$ final state is enhanced compared to the $4f^0$. The magnetic moment is suppressed, and the Kondo temperature increases. This replicates the behavior of the $5f^5$ and $5f^4$ final states, and the magnetism, in PuSi_x series.

V. CONCLUSIONS

All PuSi_x ($0.5 \leq x \leq 2.0$) silicides have localized $5f$ states. With increasing dilution, hybridization between the $5f$ states

and the Si $3p$ ligand states becomes more pronounced, as shown by the increase of the well-screened $4f$ line. For the $5f$ emission, two final-state multiplet structures were identified, corresponding to the $5f^5$ (three-peak structure close to the Fermi level) and the $5f^4$ (broad peak at 2 eV binding energy) configurations. They represent the well- and poorly screened $5f$ final states. The well-screened final state appears in the more hybridized PuSi_2 ; the poorly screened final state is observed in the less hybridized PuSi . The photoemission data agree well with the magnetic properties of the silicides. All multiplet structures are consistent with calculations, which for Pu are done in the intermediate coupling scheme.

There is a strong analogy between Pu and Ce. Photoemission from the ground-state configurations (Pu $5f^5$, Ce $4f^1$) gives either the well-screened final state at low binding energy (Pu $5f^5$, Ce $4f^1$) or the poorly screened final state at high binding energy (Pu $5f^4$, Ce $4f^0$). Similar photoemission features are observed in other metallic Pu compounds, and the question is raised whether in all these compounds final-state multiplet structures occur. Two prominent systems are PuSe , where intermediate valence ($5f^5$ - $5f^6$) leads to two final states, and δ -Pu, where part of the spectral intensity also seems to originate from the $5f^5$ final-state multiplet.

In this work, interpretation of the photoemission spectra is done qualitatively following the well-established screening model. It is hoped that it stimulates development of more quantitative models for photoemission in the actinides.

ACKNOWLEDGMENTS

We are grateful to F. Wastin and G. H. Lander for stimulating discussions.

*Electronic address: gouders@itu.fzk.de

- ¹A. L. Boring and J. L. Smith, *Los Alamos Sci.* **26**, 90 (2000).
- ²T. Gouder, L. Havela, F. Wastin, and J. Rebizant, *Europhys. Lett.* **55**, 705 (2001).
- ³T. Gouder, F. Wastin, J. Rebizant, and L. Havela, *Phys. Rev. Lett.* **84**, 3378 (2000).
- ⁴L. Havela, T. Gouder, F. Wastin, and J. Rebizant, *Phys. Rev. B* **65**, 235118 (2002).
- ⁵R. D. Baptist, D. Courteix, J. Chayrouse, and L. Heinz, *J. Phys. F: Met. Phys.* **12**, 2103 (1982).
- ⁶J. R. Naegele, J. Ghijsen, and L. Manes, *Actinides—Chemistry and Physical Properties*, Structure and Bonding Vol. 59/60 (Springer, Berlin, 1985), p. 197.
- ⁷L. E. Cox, *Phys. Rev. B* **37**, 8480 (1988).
- ⁸A. J. Arko, J. J. Joyce, L. Morales, J. Wills, J. Lashley, F. Wastin, and J. Rebizant, *Phys. Rev. B* **62**, 1773 (2000).
- ⁹T. Gouder and L. Havela, *Mikrochim. Acta* **138**, 207 (2002).
- ¹⁰J. G. Tobin, B. W. Chung, R. K. Schulze, J. Terry, J. D. Farr, D. K. Shuh, K. Heinzelman, E. Rotenberg, G. D. Waddill, and G. van der Laan, *Phys. Rev. B* **68**, 155109 (2003).
- ¹¹S. Y. Savrasov, G. Kotliar, and E. Abrahams, *Nature (London)* **410**, 793 (2001).

- ¹²J. J. Joyce, J. M. Wills, T. Durakiewicz, M. T. Butterfield, E. Guzewicz, J. L. Sarrao, L. A. Morales, A. J. Arko, and O. Eriksson, *Phys. Rev. Lett.* **91**, 176401 (2003).
- ¹³J. M. Wills, O. Eriksson, A. Delin, P. H. Andersson, J. J. Joyce, T. Durakiewicz, M. T. Butterfield, A. J. Arko, D. P. Moore, and L. A. Morales, cond-mat/0307767 (unpublished).
- ¹⁴S. Y. Savrasov and G. Kotliar, *Phys. Rev. Lett.* **84**, 3670 (2000).
- ¹⁵G. R. Stewart, *Rev. Mod. Phys.* **56**, 755 (1984).
- ¹⁶B. R. Cooper, P. Thayamballi, J. C. Spirlet, W. Müller, and O. Vogt, *Phys. Rev. Lett.* **51**, 2418 (1984).
- ¹⁷D. Malterre, M. Grioni, P. Weibel, B. Dardel, and Y. Baer, *Phys. Rev. B* **48**, 10599 (1993).
- ¹⁸J. J. Joyce, A. J. Arko, J. Lawrence, P. C. Canfield, Z. Fisk, R. J. Bartlett, and J. D. Thompson, *Phys. Rev. Lett.* **68**, 236 (1992).
- ¹⁹S. Hüffner and P. Steiner, *Z. Phys. B: Condens. Matter* **46**, 37 (1982).
- ²⁰S. Hüffner, *Photoelectron Spectroscopy, Principles and Applications* (Springer-Verlag, Berlin, 2003).
- ²¹P. Sigmund, *Nucl. Instrum. Methods Phys. Res. B* **27**, 266 (1987).
- ²²J. R. Naegele, L. Manes, J. C. Spirlet, and W. Müller, *Phys. Rev. Lett.* **52**, 1834 (1984).

- ²³G. van der Laan, *J. Electron Spectrosc. Relat. Phenom.* **117-118**, 89 (2001).
- ²⁴J. J. Yeh and I. Lindau, *At. Data Nucl. Data Tables* **32**, 1 (1985).
- ²⁵G. R. Stewart and R. O. Elliott, in Lawrence Berkeley National Laboratory Report No. LBL-12441, 1981 (unpublished), p. 206.
- ²⁶P. Boulet, F. Wastin, E. Colineau, and J. Rebizant, *J. Phys.: Condens. Matter* **15**, 2305 (2003).
- ²⁷J. C. Fuggle, M. Campagna, Z. Zolnierok, R. Lässer, and A. Plaut, *Phys. Rev. Lett.* **45**, 1597 (1980).
- ²⁸M. Campagna, G. K. Wertheim, and Y. Baer, *Photoemission in Solids II, Case Studies*, Photoemission in Applied Physics Vol. 27 (Springer-Verlag, Berlin, 1979).
- ²⁹N. Martensson, B. Johansson, and J. R. Naegele, *Phys. Rev. B* **35**, 1437 (1987).
- ³⁰F. Gerken and S. Schmidt-May, *J. Phys. F: Met. Phys.* **13**, 1571 (1983).
- ³¹G. van der Laan, K. T. Moore, J. G. Tobin, B. W. Chung, M. A. Wall, and A. J. Schwartz, *Phys. Rev. Lett.* **93**, 097401 (2004).
- ³²Y. Baer, R. Hauger, C. Zürcher, M. Campagna, and G. K. Wertheim, *Phys. Rev. B* **18**, 4433 (1978).
- ³³P. Wachter, F. Marabelli, and B. Bucher, *Phys. Rev. B* **43**, 11136 (1991).
- ³⁴B. Reihl, *J. Less-Common Met.* **128**, 331 (1987).